3) Combining these two highly simplified relationships leads to the scaling law suggested by the results in Fig. 1, namely that

$$W_T \propto W_p^{2/3}$$

4) Other effects, such as the method of propellant confinement, method of tank rupture, and ignition delay time, appear to be secondary to this basic scaling trend and are undoubtedly, the source of significant and, indeed, predictable[6] variation about the mean trend.

Although only a portion of the Project PYRO results were utilized for Fig. 1, they are considered representative of the general trend. This trend permits a reasonable and conservative estimate of the possible explosion magnitude. With this in mind, the following additional information is obtained from Fig. 1.

1) The maximum trend for the PYRO data, shown by the vertical bars through the data for $W_p = 200$, 1000, and 25,000 lb, lies roughly on a similar two-thirds power scaling trend line and indicates a maximum probable yield of about 2.2 times the average yield.

2) Based on the two-thirds scaling law, the data suggest that the maximum yields observed in the PYRO tests were about 7.3 times greater than the average (scaled) yield estimated for the three actual accidents.

For comparison, dashed lines corresponding to previous design rules of 20% and 60% TNT yield are shown on the figure. It is clear that the 20% or 60% TNT equivalent rules would lead to very conservative estimates of the TNT equivalency for large amounts of propellant. Clearly, these earlier constant percentage rules for TNT yield are not consistent with the experimental data cited in Fig. 1. The simple two-thirds power law shown appears to provide an improved empirical model for initial estimates of the TNT equivalence of LOX/LH_2 propellants over a wide range of propellant weights. The data suggest that a scaling law for the maximum TNT equivalent for these propellants can be given by $W_T \simeq 4W_P^{2/3}$. This is the principal result of this Note. The empirically determined scaling constant (4) may vary substantially for other types of propellants. However, it is estimated to be a reasonable maximum value for LOX/LH_2 propellant explosions from a variety of tank configurations and failure modes, which were demonstrated very well by the experimental studies considered here.[2,3]

Another scaling principle, based on thorough analytical and laboratory studies on propellant explosions by Farber,[5] is partly verified by the data in Fig. 1. This principle is based on the concept of self-ignition of LOX/LH_2 propellants by a "critical mass" equivalent to a TNT weight of about 4000 lb. This upper bound, indicated by the shaded bar in Fig. 1, appears to correspond approximately to the maximum yield observed in the data. Further investigation of these useful scaling principles seems warranted in order to expand the spectrum of prediction tools available for planning liquid propellant facilities—ranging from the type of simple empirical scaling law suggested herein to the more accurate methods reported by Baker et al.[6]

References

[1] Joint Army-Navy-NASA-Air Force (JANNAF) Hazards Working Group, "Chemical Rocket/Propellant Hazards—Volume I, General Safety Engineering Design Criteria," Chemical Propulsion Information Agency (CPIA) Publication 194, Oct. 1971.

[2] "Liquid Propellant Explosive Hazards—Project PYRO," Air Force Rocket Propulsion Lab., AFRPL-TR-68-92, Vols. I, II, and III, Dec. 1968.

[3] "Statistical Analysis of Project PYRO Liquid Propellant Explosion Data," Bellcomm, Inc., 1969.

[4] "Solid Propellant Explosive Test Program—Project SOPHY," Aerojet General Corp., AFRPL-TR-67-211, Vols. I and II, Aug. 1967.

[5] Farber, E.A., "Prediction of Explosive Yield and Other Characteristics of Liquid Propellant Rocket Explosions," NASA Contract NAS 10-1255, Final Report, University of Florida, Gainesville, Fla., Oct. 1968.

[6] Baker, W.E. et al, "Workshop for Predicting Pressure Wave and Fragment Effects of Exploding Propellant Tanks and Gas Storage Vessels," NASA CR-134906, Southwest Research Institute, Nov. 1975.

[7] Weiss, H., personal communication, Rocketdyne Div., North American Rockwell Corp., Canoga Park, Calif., May 1971.

Radiative Heat Transfer within a Solid-Propellant Rocket Motor

Blaine E. Pearce*
The Aerospace Corporation, El Segundo, Calif.

Introduction

THIS Note presents an approximate description of the radiative heat transfer between the two-phase combustion products and walls within a solid-propellant rocket motor. The study was motivated by the absence of a description that correctly accounts for scattering by the aluminum oxide (Al_2O_3) particles. Previous studies[1] and the model currently used within the industry are incorrect in this respect. The radiative transfer model proposed here correctly accounts for scattering but ignores the nonhomogeneous, nonisothermal structure of the two-phase flow. This simplification implies that the model is most accurate in the low subsonic Mach number region of the nozzle. In spite of its approximate nature, it is argued that the model is sufficiently accurate for its intended purpose; moreover, the accuracy is commensurate with our present knowledge of sizes and optical properties of actual particles in a rocket exhaust.

Radiative Transfer Solution

The axisymmetric flow of the two-phase exhaust products is modeled as a homogeneous and isothermal circular cylinder with a diameter equal to the local nozzle diameter and a temperature and particle density equal to the local average values. Particles in the flow absorb and are assumed to scatter radiation isotropically. A radiative transfer solution is constructed using the diffusion approximation for the mean (with respect to all directions) intensity. A general derivation of this approximation and a solution for plane layers are given by Edwards and Bobco.[2] Adzerikho and Nekrasov[3] have applied it to a cylinder and sphere.

The result of the radiative transfer solution which is applicable to heat-transfer predictions is the hemispherical emissivity $E(\tau_R, \omega)$ of the cylinder with radius R, optical radius $\tau_R = \kappa^{(e)}R$, and albedo for single scattering $\omega = \kappa^{(s)}/\kappa^{(e)}$. The results of the calculation are summarized in Table 1 which gives the hemispherical emissivity for single-scattering albedos applicable to Al_2O_3 particles. Although the radiative transfer formulation is approximate, it is highly accurate, giving a hemispherical emissivity that underpredicts the exact value[4] (last row, Table 1) with an error less than 4% for

Received June 27, 1977; revision received Dec. 16, 1977.

Index categories: Radiation and Radiative Heat Transfer; Multiphase Flows.

*Member of the Technical Staff, Aerothermodynamics Dept.; presently, Consultant, Aeronautical Research Associates of Princeton, Inc., Princeton, N. J. Member AIAA.

Table 1 Emmisivity of a homogeneous, absorbing, and isotropically scattering circular cylinder, $E(\tau_R, \omega)$

τ_R	$\omega=0$	0.6	0.8	0.85	0.9	0.925	0.95	0.975	0.99
0.02	0.3948(−1)[a]	...[b]	...	...	...	...	...	...	...
0.05	0.9436(−1)	0.3918(−1)	...	...	...	...	...	...	...
0.1	0.1774	0.7551(−1)	0.3878(−1)	0.2936(−1)	0.1984(−1)	...	...	...	...
0.2	0.3176	0.1424	0.7436(−1)	0.5647(−1)	0.3820(−1)	0.2893(−1)	0.1955(−1)	...	...
0.5	0.5962	0.3066	0.1697	0.1308	0.8977(−1)	0.6839(−1)	0.4639(−1)	0.2375(−1)	0.9846(−2)
1.0	0.8144	0.4920	0.2980	0.2361	0.1669	0.1292	0.8897(−1)	0.4615(−1)	0.1907(−1)
2.0	0.9458	0.6667	0.4598	0.3825	0.2868	0.2297	0.1644	0.8892(−1)	0.3762(−1)
5.0	0.9923	0.7634	0.5940	0.5265	0.4353	0.3743	0.2949	0.1830	0.8661(−1)
10.0	0.9981	0.7817	0.6243	0.5628	0.4805	0.4259	0.3544	0.2476	0.1380
20.0	0.9995	0.7887	0.6363	0.5768	0.4977	0.4455	0.3776	0.2775	0.1747
50.0	0.9999	0.7921	0.6424	0.5840	0.5066	0.4554	0.3891	0.2918	0.1927
100.0	1.000	0.7921	0.6424	0.5840	0.5066	0.4558	0.3899	0.2933	0.1952
∞(exact)	1.0000	0.8053	0.6581	0.5998	0.5220	0.4704	0.4033	0.3056	...

[a] $0.3948(-1) = 0.3948 \times 10^{-1}$.
[b] The optically thin limit applies to the blank entries, for which $E(\tau_R, \omega) = 2(1-\omega)\tau_R$.

$\tau_R \to \infty$.† A comparison with exact solutions for neutron transport in a cylinder shows the same magnitude of error at intermediate optical depths.[5] In addition to the tabulated numerical results for intermediate τ_R, it is useful to give the limiting cases:

$$\lim_{\tau_R \to 0} E(\tau_R, \omega) = 2(1-\omega)\tau_R \tag{1}$$

$$\lim_{\tau_R \to \infty} E(\tau_R, \omega) = 1 - \frac{2\omega[(1/k) - (1/k^2)\ln(1+k)]}{1 + \frac{2}{3}k}$$

$$k^2 = 3(1-\omega) \tag{2}$$

The net radiative heat transfer between the wall and the cylinder volume can then be written as

$$q = \frac{B - B_w}{1/\epsilon_w + 1/E(\tau_R, \omega) - 1} = \epsilon_{\text{eff}}(B - B_w) \tag{3}$$

where B and B_w are the blackbody emissive powers at the exhaust products and wall temperature, respectively. This equation defines an effective emissivity (either spectral or total) for the exchange between the wall and cylinder volume.

Application to Solid-Propellant Rockets

An application of the radiative transfer solution to an actual solid-propellant exhaust requires an integration over a particle size distribution and also wavelength. Let $n(r)$ be the normalized particle number density distribution‡ with respect to particle radius. The size-averaged optical coefficient [for extinction $\kappa^{(e)}$, scattering $\kappa^{(s)}$, and absorption $\kappa^{(a)}$] is

$$\bar{\kappa}_\lambda{}^{(\alpha)} = N\pi \int_0^\infty n(r) r^2 Q_\lambda^{(\alpha)}(r)\, dr \qquad \alpha = e, s, a, \tag{4}$$

where Q_λ is the efficiency (optical cross section normalized by the geometric cross section, πr^2). The total number density is

$$N = \frac{\rho_p}{(4/3)\pi\rho_s} \int_0^\infty n(r) r^3\, dr \tag{5}$$

where ρ_p and ρ_s are the particle density in the exhaust products and the solid particle density, respectively. Optical cross sections for the range of particle sizes and wavelengths of importance [$2\pi r/\lambda = O(1)$] must be computed for the Mie theory for spherical homogeneous particles using one of the more recent tabulations of the complex index of refraction.[6]

In order to illustrate the use of the radiative transfer solution, the heat transfer will be computed for the specific case of the 7.62-cm (3-in.) radius geometric throat of a 160-kN (35,000 lb_f) thrust motor using an 86% solids, 18% Al (86/18) HTPB propellant. The particle temperature is 3100 K, and a wall temperature of 2800 K (typical of a carbon or graphite material) is assumed. For this calculation a particle size distribution of the form

$$n(r) = \frac{a^{b+1} r^b e^{-ar}}{\Gamma(b+1)} \tag{6}$$

is used with $a = 3.0\ \mu\text{m}^{-1}$, $b = 2$, for which the mass mean radius $r_{43} = 2.0\ \mu$m. This assumed distribution is believed to be typical of that for motors of this size, based on samples captured outside the motor. The net heat transfer to the wall (assumed black, $\epsilon_w = 1$) for this particular case is

$$q = \int_0^\infty E(\bar{\tau}_{R\lambda}, \bar{\omega}_\lambda)\,[B_\lambda(T) - B_\lambda(T_w)]\, d\lambda = 75.5\ \text{W/cm}^2 \tag{7}$$

The heat flux between opaque black surfaces at these temperatures is $\sigma(T^4 - T_w^4) = 175\ \text{W/cm}^2$, so the effective emissivity of the scattering-cylinder/black-wall combination is 0.43. A convective heat flux through a turbulent boundary layer of $\sim 550\ \text{W/cm}^2$ is predicted for this location. Radiation from the particles thus contributes only about 12% of the total heat flux in this example. This conclusion is expected to obtain for most solid rocket motors. Upstream, radiation is expected to be a larger fraction of the heating because the radiation flux increases (higher particle temperature), while the convective heating decreases (reduced heat-transfer coefficient). In the combustion chamber radiation is expected to be the dominant heating mechanism.

Particle extinction occurs most strongly at short wavelengths which coincide with the spectral region where most of the radiant energy is contained at temperatures typical of the subsonic portion of the flow. For example, at 3000 K, 74% of the radiation occurs at $\lambda \leq 2\mu$m. In contrast, most emission from the gaseous species H_2O, CO_2, CO, and HCl in the propellant exhaust occurs at $\lambda > 2.2\mu$m. This spectral separation allows the gaseous radiation to be calculated essentially independently of that from the particles. Moreover, an upper bound estimate of the gaseous contribution to the wall heat flux is only about 15% of that due to the particles in this specific example. Again, this result is

†Adzerikho and Nekrasov[3] give an approximate analytical solution for $E(\tau_R, \omega)$. However, their result for a cylinder does not approach a common value for the slab and sphere as $\tau_R \to \infty$, as is required, and an error of as much as 20% is quoted. The results presented here were obtained by a careful numerical quadrature of the exact expression for $E(\tau_R, \omega)$ and do coincide with the slab solution as $\tau_R \to \infty$.

‡Normalized such that $\int_0^\infty n(r)\, dr = 1$.

expected to apply to most solid rocket motors. Particles thus will be the dominant radiation source until the exhaust cools sufficiently to shift a significant fraction of the spectral energy distribution to wavelengths where the gaseous species radiate ($T < 1500$ K).

Comparison of Scattering Solution with Empirical Emissivity and Experimental Intensity Measurements

An empirical specification of the emissivity of a solid-propellant rocket exhaust flow near the nozzle throat is currently used:[7]

$$E = 1 - e^{-2\mu R} \tag{8}$$

where $\mu = 0.808\,(n/16)\,\rho$ (n = % Al in propellant, ρ = exhaust density in lb_m/ft^3, and R is the local radius in inches). The functional form of this expression is appropriate for a purely absorbing flow. For example, as $\mu R \to \infty$, $E \to 1$, which is not the correct limit for scattering volume (see Table 1). Comparison between the scattering solution and the empirical emissivity is made here for the 86/18 HTPB propellant and for various nozzle diameters. The empirical specification gives $\mu = 0.059$ cm^{-1} and evaluation of the optical properties for the size distribution of particles given by Eq. (6) gives an average (with respect to size and wavelength) $\bar{\kappa}^{(e)} = 2.50$ cm^{-1} and $\bar{\omega} = 0.925$. The comparison is shown in Fig. 1 and indicates that the empirical equation can overestimate the heat flux by as much as a factor of 2 (as $\mu R \to \infty$). More importantly, the empirical equation indicates a much greater sensitivity of the radiation to motor size, Al content, or chamber pressure than does the more correct scattering solution. Although radiation heating is less important than convection in the nozzle, the fact that radiative heating is indicated by the scattering solution to be nearly insensitive to motor size for nozzles larger than a few cm in diameter may be of importance in rationalizing heat-transfer and thermochemical ablation measurements made during test firings of motors that differ greatly in size, chamber pressure, or Al content.

The experimental[8] data upon which Eq. (8) was based are the only direct measurements of radiation within a solid propellant motor known to the author. These measurements consist of emission from the optical path across the throat diameter (3.18 cm) of an actual small-scale rocket motor. Measurements of the emerging intensity were made with a wide band radiometer and two narrow spectral bandpasses

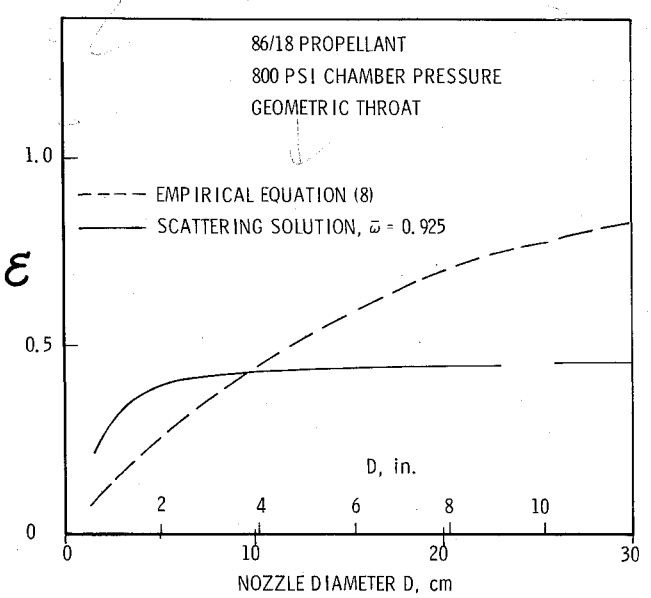

Fig. 1 Hemispheric emissivity at the nozzle throat.

Table 2 Comparison of measured and predicted brightness temperatures

Propellant properties (at TM-3 motor throat, $D = 3.18$ cm)		
UTP 1090 propellant 16% Al, $T = 3197$ K $p = 27.23$ atm $\rho_p = 8.45 \times 10^{-4}$ g/cm^3 (particle density in exhaust)		
Summary of measurements and predictions		
	Brightness temperatures, K	
λ, μm	Measured[8]	Predicted
0.506	2704	2860
0.643	2578	2690
$0 \to \infty$	2200	2405

centered at $\lambda = 0.506$ and 0.643 μm and converted to brightness temperatures by comparison with calibrated sources. The radiant intensity for a line of sight across the diameter was computed using the radiative transfer solution proposed here for the propellant properties given in Table 2. Several particle size distributions of the form given by Eq. (6) with $1.125 \leq r_{43} \leq 2.25$ μm were used and optical properties at the short wavelengths were taken from Ref. 9. The calculated brightness temperatures were found to be essentially insensitive to the size distribution and the mean values are compared with the measured temperatures in Table 2. The predictions are uniformly too high, but the error (< 10%) is sufficiently small to suggest that the radiative transfer model is essentially verified, at least for this particular case.

Discussion and Conclusions

The essential simplification made in the proposed model is to ignore the spatial nonhomogeneous and nonisothermal structure of the actual flow. The error in this approximation is unknown; however, it is expected to be small in the subsonic portion of the flow. One aspect of the real flow, the effect of the large temperature gradient in the wall turbulent boundary layer, was assessed.[10] The thermal boundary layer was found to diminish the wall heat flux by only a few percent for the thermal layer thickness ($\delta_{th} < 0.25$ cm) typical of solid rocket motors.

Another assumption of potential importance concerns isotropic scattering. Real Al_2O_3 particles scatter highly anisotropically. An assessment of this effect was made using a linearly anisotropic scattering law.[10,11] For the extreme case of forward scattering allowed by this law (which is not as severe as that for real particles), the wall heat flux is increased by as much as 14%. Thus the radiative transfer solution given here will underpredict the heat transfer due to this assumption.

The essential conclusions allowed by the radiative transfer model and specific calculations given here are that most solid rocket exhaust flows are optically thick in the subsonic portion of the flow for all but the smallest motor, lowest chamber pressures, or lowest Al content propellants. Radiation is the dominant heat flux only in the combustion chamber, and drops to only a small fraction of the convective heat flux near the nozzle throat. Radiation from the particles is large compared to that from the gaseous species. Because the simple model proposed here seems to provide a valid estimate of the radiative heating, and because of the small contribution of radiation to the total heating within the nozzle, it is suggested that more refined calculations may not be warranted at this time.

Acknowledgment

Phil Henderson of United Technologies/Chemical Systems Division kindly provided Ref. 8.

References

[1]Byrne, W.M. Jr., "Radiant Heat Transfer to an Enclosure from Two-Phase Flows," *Journal of Spacecraft and Rockets,* Vol. 3, June 1966, pp. 919-924.

[2]Edwards, R.H. and Bobco, R.P., "Radiant Heat Transfer from Isothermal Dispersions with Isotropic Scattering," *Journal of Heat Transfer, Transactions of ASME,* Ser. C, Vol. 89, Nov. 1967, pp. 300-308.

[3]Adzerikho, K.S. and Nekrasov, V.P., "Luminescence Characteristics of Cylindrical and Spherical Light-Scattering Media," *International Journal of Heat Mass Transfer,* Vol. 18, Oct. 1975, pp. 1131-1138.

[4]Chandrasekhar, S., *Radiative Transfer,* Dover, New York, 1960, pp. 327-328, Table XXXIII.

[5]Stuart, G.W., "Multiple Scattering of Neutrons," *Nuclear Science and Engineering,* Vol. 2, Sept. 1957, pp. 617-625.

[6]Gal, G. and Kirch, H., "Particulate Optical Properties in Rocket Plumes," Air Force Rocket Propulsion Laboratory, Rept. AFRPL-TR-73-99, Nov. 1973.

[7]Murphy, A. and Kwong, K., *Nozzle Control Bulletin,* Acurex Aerotherm Corporation, Aerotherm Rept. TM-75-86, Nov. 1975.

[8]Alport, J.J., "Results of a Measurement of the Emissivity and Temperature of the Combustion Products in the Throat of a TM-3 End Burning Motor," United Technology Corporation, TM-33-68-U1, June 9, 1961.

[9]Mularz, E.J. and Yuen, M.C., "An Experimental Investigation of Radiative Properties of Aluminum Oxide Particles," *Journal of Quantitative Spectroscopy and Radiative Transfer,* Vol. 12, Nov. 1972, pp. 1553-1568.

[10]Pearce, B.E., "Radiative Heat Transfer Within a Solid Propellant Rocket Motor," The Aerospace Corporation, Rept. No. TOR-0077 (2451-10)-5, July 25, 1977.

[11]Dyan, A. and Tien, C.L., "Heat Transfer in a Gray Planar Medium with Linear Anisotropic Scattering," *Journal of Heat Transfer,* Vol. 97, Aug. 1975, pp. 391-396.